Synthesis, Spectroscopic Interpretations, and Antioxidant Efficiency of Two Vital Selenium Complexes

F.A.I. Al-Khodir*

Department of Chemistry, College of Science, Princess Nora Bint Abdul Rahman University, Riyadh, Saudi Arabia

This paper aimed to synthesis, spectroscopic characterizations, and antioxidant assessment of two new selenium complexes with nicotinamide (Nic) and riboflavin (RF) as drug chelates. The speculated structures of the synthetic selenium complexes have been discussed by using different tools of spectroscopic analyses like infrared, the Raman, electronic, ^{1}H-NMR, and mass. Accordingly, the Fourier transform infrared and ^{1}H-NMR spectra, the mode of complexation is supported, as four molecules of nicotinamide drug act as a monodentate chelate through the N-atom of the pyridine ring with $[Se(Nic)_4]\cdot H_2O$ formula. The two riboflavin drug molecules coordinated to selenium metal as a bidentate chelate through azomethine nitrogen of pyrazine ring and O-atom of C=O pyrimidine-2,4-dione group with general formula $[Se(RF)_2]$. Both of Nic and RF chelates act as neutral charge ligands. The conductivity measurements indicated that the selenium complexes are non-electrolytes behaviors. Thermal analyses (thermal gravimetric-differential thermal analysis) of the studied complexes show that the decomposition process takes place in one broadening step with a wide temperature range. The surface morphology of the mentioned complexes was studied by scanning electron microscope and the particle size is calculated using X-ray powder diffraction. Thermodynamic kinetic parameters are calculated by using the Coats and Redfern equation. Screening of antioxidant activities of selenium complexes *in vitro* are assessed. The antioxidant activity is studied by three methods (DPPH assay, β-carotene/linoleic acid bleaching assay, and ferric reducing power assay), the studied complexes have a significant antioxidant activity compared to synthetic antioxidants like trolox and BHT.

1. Introduction

Selenium element and organoselenium play an essential role in the biological systems [1–7]. Generally, metal ions were required for many critical functions in humans [8–10]. Metal complexes have played key role in the development of modern chemotherapy [11–14], however, the study of metal–drug complexes is still in its early stages, thus representing a great challenge in current synthetic chemistry and coordination chemistry.

Nicotinamide namely vitamin B_3 (Fig. 1A) has been demonstrated as anti-inflammatory actions and anti-cancer agent [15, 16]. Some transition metal complexes of nicotinamide have been discussed both structurally and spectroscopically [17–24]. Riboflavin (Fig. 1B) is a member of vitamins (B complex) that is an important antioxidant agent. There is little attention in the literature about the complexation of RF [25–27]. For the first time Malele et al. [26] synthesized and characterized RF–Mo(V) complex in powder form using $[Mo_2O_4(H_2O)_6]^{2+}$ complex as a precursor for the synthesis.

Vitamins have a number of essential functions in the body, main role is as an antioxidant. It protects body cells from toxic compounds, heavy metals, such as lead and cadmium, and also from the side effects of drugs, radiation and free radical damage. This research aims
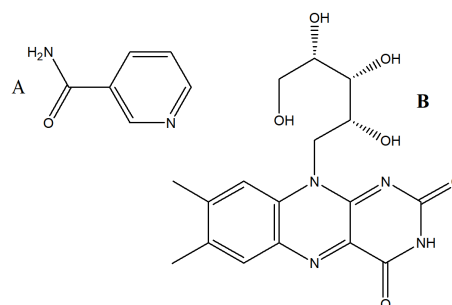
*e-mail: fatimaalkhodir@yahoo.com

Fig. 1. Structures of nicotinamide (A) and riboflavin (B) drugs.

to prepare new selenium compounds with in *vitro* screening of antioxidant properties by combining the selenium element in a metallic state with both nicotinamide and riboflavin vitamins to form an antioxidant pharmacological model. There are little spectroscopic characterizations and thermal stability about the chemical interaction between vitamin drugs and selenium metal.

2. Experimental

2.1. Reagents

All chemicals used throughout this study were Analar or extra pure grade and received from Aldrich chemical company. The selenium metal, nicotinamide, and riboflavin used in this paper were of analytical grade and used without further purification. The solvents were used without distillation. 2,2-diphenyl-1-

picrylhydrazyl (DPPH), methanol, *n*-hexane, 2-deoxy-2-ribose, β-carotene and linoleic acid, were procured from Sigma (Sigma-Aldrich GmbH, Sternheim, Germany). Tween 40 and dimethyl sulphoxide (DMSO) were from Merck (Darmstadt, Germany).

2.2. Synthesis of Nic and RF selenium complexes

A mixtures of solid powder of selenium metal (4 mmol) with nicotinamide (16 mmol) or riboflavin (8 mmol) in toluene solvent (50 mL) were refluxed for 24 h at 60 °C. The unreacted selenium metal powder was removed by filtration, and the color resultants solutions were reduced to *ca.* 1/3 of its volume and cooled to room temperature. The solid complexes obtained were then collected by filtration, washed with little amount of toluene and dried in *vacuo* over anhydrous calcium(II) chloride. The purity was checked by thin layer chromatography.

2.3. Instruments

The micro-analytical analyses of %C and %H percentages were calculated using a Perkin Elmer CHN 2400 (USA). The metal content was determined gravimetrically by converting the compounds to its corresponding stable form. The molar conductivity of the two selenium complexes with 10^{-3} mol/cm^3 concentration in DMSO solvent was measured using Jenway 4010 conductivity meter. The UV-vis absorption spectra were recorded in DMSO solvent within 800–200 nm range using a UV2-Unicam UV/Vis Spectrophotometer fitted with a quartz cell of 1.0 cm path length. The infrared spectra with KBr discs were recorded on Bruker FT-IR Spectrophotometer (4000–400 cm^{-1}), while Raman laser spectra of samples were measured on the Bruker FT-Raman with laser 50 mW. The thermal studies (thermogravimetric/differential thermal gravimetric, TG/DTG–50H) were carried out on a Shimadzu thermogravimetric analyzer under nitrogen till 800 °C. All experiments were performed using a single loose top loading platinum sample pan under nitrogen atmosphere at a flow rate of 30 mL/min and a 10 °C/min heating rate for the temperature range 25–800 °C. ^{1}H-NMR spectra were recorded as DMSO solutions on a Bruker 600 MHz spectrometer using TMS as the internal standard. Scanning electron microscopy (SEM) images were obtained using a JEOL Jem-1200 EX II electron microscope at an acceleration voltage of 25 kV. X-ray diffraction (XRD) patterns of the sample was recorded on X Pert Philips X-ray diffractometer. All the diffraction patterns were obtained by using Cu $K_{\alpha 1}$ radiation, with a graphite monochromator at 0.02°/min scanning rate.

2.4. Anti-oxidative assays

The antioxidant activity of selenium complexes were measured in terms of hydrogen-donating or radical-scavenging ability, using the stable radical DPPH as a reagent [28]. The β-carotene/linoleic acid bleaching assay was determined by measuring the inhibition of selenium complexes and conjugated diene hydroperoxides arising from linoleic acid oxidation by described method [29]. The reductive potential based on the ferric reducing antioxidant power of the studied complexes and the standards positive controls (BHT and trolox) was determined [30]. Each of the measurements described was carried out in three replicate experiments and the results are recorded as mean±standard deviation. The significantly different calculated at level of $p \leq 0.05$.

2.5. Thermodynamic activation parameters

The thermodynamic activation parameters of decomposition processes of Nic and RF selenium complexes namely activation energy (E^*), enthalpy (ΔH^*), entropy (ΔS^*) and Gibbs free energy change of the decomposition (ΔG^*) were evaluated graphically by employing the Coats–Redfern relation [31]. The entropy of activation (ΔS^*), enthalpy of activation (ΔH^*) and the free energy change of activation (ΔG^*) were calculated using the following equations:

$$\Delta S^* = 2.303(\log(Ah/kT)R, \tag{1}$$

$$\Delta H^* = E^* - RT, \tag{2}$$

$$\Delta G^* = \Delta H^* - T\Delta S^*. \tag{3}$$

3. Results and discussion

3.1. Micro-analytical and physical study

The analytical, physicochemical results and spectroscopic outcome are in a good agreement with the speculated structures of mentioned two selenium complexes. The elemental analyses data of the selenium complexes of nicotinamide and riboflavin reveal that the two complexes have 1:4and 1:2 stoichiometry (metal:ligand), respectively. The resulting selenium complexes are soluble in DMSO and DMF with gently warming but insoluble with alcohols and other organic solvents. The physicochemical results like color, yield, melting point as well as molar conductance values of these complexes are listed in Table I. At room temperature, the conductance data of the selenium complexes which dissolved in DMSO are existing within 12–14 Ω^{-1}cm^{2}mol^{-1} range, these data confirm that the two prepared selenium complexes are non-electrolytes [32]. The speculated structures of both selenium complexes with Nic and RF are represented in Fig. 2.

TABLE I

Physical data: color, melting point [°C], Λ_m [Ω^{-1}cm^{2}mol^{-1}], yield, and elemental analysis %found/(%calc.) of Se(IV) folate complex.

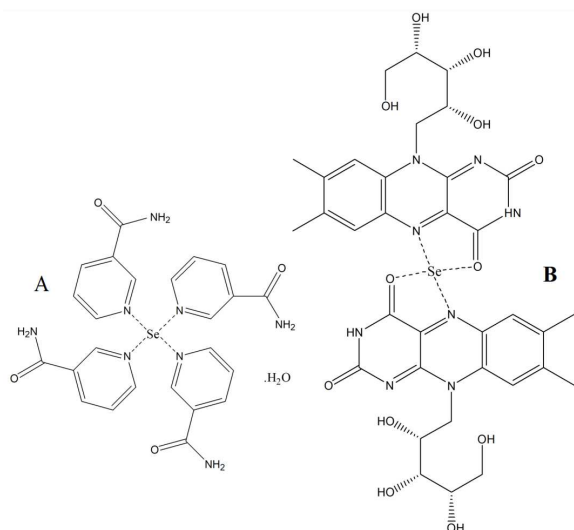| Empirical formula	Color	M.P.	Λ_m	Yield	C	H	Se
[Se(Nic)$_4$].H$_2$O	light pink	279	12	84	49.27 (49.23)	4.40 (4.48)	13.43 (13.49)
[Se(RF)$_2$]	yellow	320	14	88	49.08 (49.10)	4.72 (4.85)	9.44 (9.49)

Fig. 2. (A) The speculated formula of selenium nicotinamide complex, (B) the speculated formula of selenium riboflavin complex.

3.2. Infrared and Raman spectra

The infrared spectra of the nicotinamide and riboflavin selenium complexes (Fig. 3) are compared with that of the Nic and RF as free ligands to notify the changes that might have taken place during the complexation (Tables II and III).

The FT-IR spectrum of $[Se(Nic)_4] \cdot H_2O$ complex is shown in Fig. 3 and its spectral data (Table II) are as-
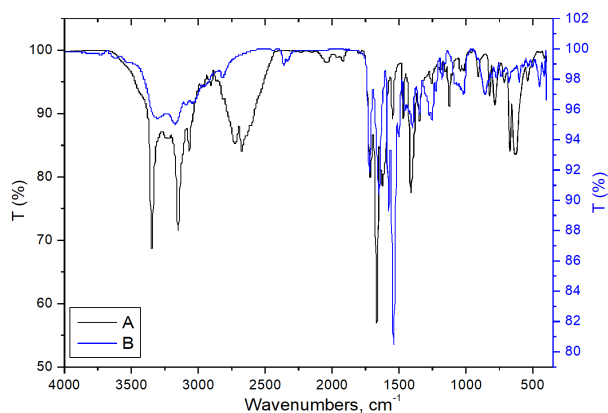
Fig. 3. FT-IR spectrum of (A) $[Se(Nic)_4] \cdot H_2O$ and (B) $[Se(RF)_2]$ complexes.

signed to give an idea about the place of the coordination between the selenium metal and Nic ligand. The infrared spectrum of Nic selenium complex shows bands at 3345 cm^{-1} which is not existed in the free chelate, that this band is assigned to the $\nu(\text{O–H})$ stretching vibration motion of uncoordinated water molecule. The stretching vibration motion $\nu(\text{N–H})$ of –NH$_2$ group is presented at 3150 cm^{-1} in case of complex form, this supported that it is not participated in the coordination process. The shifted in the wave numbers of the pyridine ring gave

Assignment of IR spectral data of Nic and $[Se(Nic)_4] \cdot H_2O$ complex.

Compound	ν(OH)	ν(NH)	ν(CH)	ν(C=O) ν(C=C) ν(C=N)		Se–N
Nic	–	3200	3060 2787 2777 2765	1699 1681 1621 1593 1576 1486 1423 1404 1396 1341 1254 1232		
$[Se(Nic)_4] \cdot H_2O$	3345 3250	3221	3068 2972 2904 2723	1715 1666 1624 1549 1467 1411 1347 1257		539 415

TABLE III

Assignment of IR spectral data of RF and $[Se(RF)_2]$ complex.

Compound	ν(OH) ν(NH)	ν(CH)	ν(C=O) ν(C=C) ν(C=N)	Se–N
RF	3372 3362 3180	3112 2935	1732 1716 1649 1622 1581 1548 1505 1459 1436 1398 1369 1346	
$[Se(RF)_2]$	3304 3172	3043 2817	1722 1649 1577 1542 1502 1401 1347	601 538 451 417

an indication about the formation of bond between the nitrogen of pyridine ring and selenium metal [33].

The infrared spectrum of the $[Se(RF)_2]$ complex (Fig. 3) is compared with its RF free ligand to notify the changes occurring during the complexation (Table III). In case of free RF ligand, the bands at (1732 and 1716 cm^{-1}) and 1548 cm^{-1} are corresponding to the stretching vibrations of C=O amide group and C=N of conjugated system, respectively. These frequencies are shifted or absent in complexation state, due to the involvement of the C=O and C=N in coordination process [33]. The free RF ligand and its selenium complex have an intense peak at 3172 cm^{-1}, which is assigned to stretching frequency of –NH group attached with the heterocyclic ring. This interpretation confirms that the –NH group is free from the sharing in the complexation. The IR spectrum of the RF selenium complex has a broadening band at 3304 cm^{-1}, which is assigned to the stretching band of O–H group.

The Raman spectra of Nic and RF selenium complexes are assigned and illustrated in Fig. 4. The Raman spectra are found to be a complementary with infrared spectroscopic techniques. The two new bands which are exhibited in both infrared and Raman spectra at around
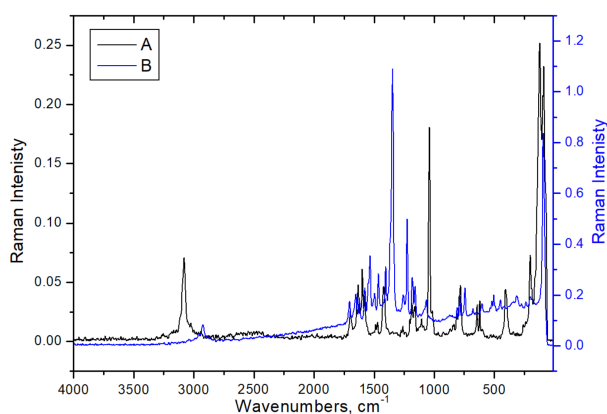
Fig. 4. Raman spectrum of (A) [Se(Nic)$_4$]·H$_2$O and (B) [Se(RF)$_2$] complexes.

600 and 400 cm^{-1}, respectively are assigned to ν(M–O) and ν(M–N), that refer to binding of selenium ions with oxygen and nitrogen atoms.

3.3. Electronic spectra

Figures 5 and 6 refer to the electronic (UV-vis) spectra of the Nic and RF selenium complexes, respectively. The nicotinamide chelate has absorption spectra in the
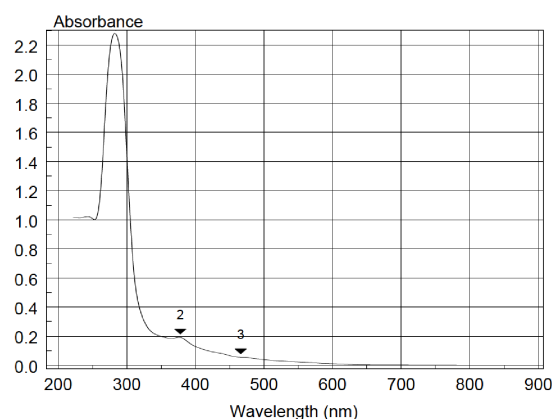

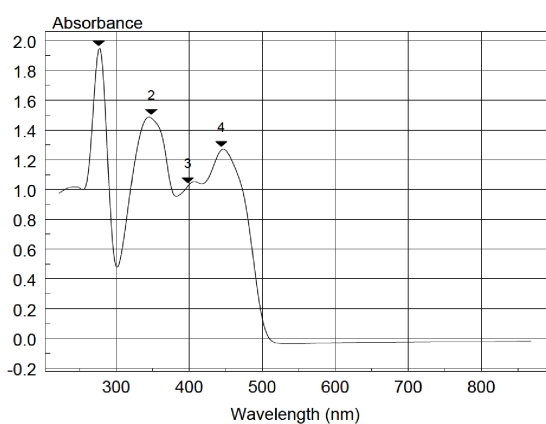Fig. 5. Electronic spectrum of Se(IV)Nic complex.

Fig. 6. Electronic spectrum of Se(IV)RF complex.

ultraviolet region in the region of the 200–400 nm and in some cases these bands extends over to higher wavelength region due to conjugation. But upon complexation with selenium metal, due to interaction with the metal ion there will be an interesting change in the electronic properties of the system. New bands in the visible region due to charge transfer spectra from metal to ligand (M–L) or ligand to metal (L–M) can be observed and this data can be processed to obtain information regarding the structure of the complexes [34]. Electronic spectrum of [Se(Nic)$_4$]·H$_2$O complex was recorded in DMSO with 10^{-3} mol/cm^3. UV-visible peaks corresponding to the $\pi \rightarrow \pi^*$ transition in the Nic complex was observed at 284 nm [35]. The peak belonging to $n \rightarrow \pi^*$ transition is recorded at wavelength 378 nm [36]. The first range can be assigned to $\pi \rightarrow \pi^*$ transitions in the aromaticity of pyridine ring while the second range is most probably due to the $n \rightarrow \pi^*$ transitions of NH$_2$ and carbonyl of amide group beside to nitrogen atom of pyridine ring [37]. The third type of transition in visible region located at 466 nm can be attributed to the ligand-to-metal charge transfer bands LM$_{CT}$ from the electronic lone pairs of pyridine nitrogen to the metal ions [38].

The absorption spectrum of RF free chelate exhibits four peaks [39] at 223, 267, 375, and 444 nm, respectively. The first two bands are due to $\pi \rightarrow \pi^*$ transitions but the other two bands at 375 and 444 nm are assigned to $n \rightarrow \pi^*$ transitions. After complexation, the spectrum of [Se(RF)$_2$] complex has four absorption bands at 276, 384, 398, and 444 nm with a red shift due to coordination towards selenium metal.

3.4. ^{1}H-NMR spectra

The ^{1}H-NMR spectrum of free nicotinamide chelate displays four chemical shifts at $\delta = 9.081$, 8.735, 8.249, and 7.527 ppm due to 4H of pyridine ring and two other peaks at $\delta = 8.22$ and 7.67 ppm which are corresponding to 2H of –NH$_2$ amido group. The ^{1}H-NMR spectrum of [Se(Nic)$_4$]·H$_2$O complex (Fig. 7) has some peaks at ($\delta = 8.528$, 8.702, 8.717, 8.905, 8.914, and 9.212 ppm), ($\delta = 7.909$, 7.921, and 7.936 ppm), $\delta = 5.831$ ppm due to 4H of pyridine ring, 2H of –NH$_2$ and 2H of H$_2$O, respectively. This results indicates that the coordination take place through –N atom of pyridine ring and far away of both –N and –O atoms of amido group. The presence of new chemical shift at 5.831 ppm due to 2H of water molecule support the located of uncoordinated water molecule outside the coordination sphere.

^{1}H-NMR spectrum of riboflavin free chelate in DMSO-d_6 refer to distinguishing of peaks for the imide proton that is observed at 11.34 ppm, aromatic protons are at 7.92 ppm, methyl groups are observed at 3.64 ppm and 2.41 ppm, protons of the side chain including the O–H protons are observed in the range from 2.50–5.14 ppm. In case of ^{1}H-NMR spectrum of [Se(RF)$_2$] complex (Fig. 8), the protons of aromatic rings, methyl groups, O–H protons are observed with small chemical shifts and the proton of –NH imide group is still unshifted which exhibited

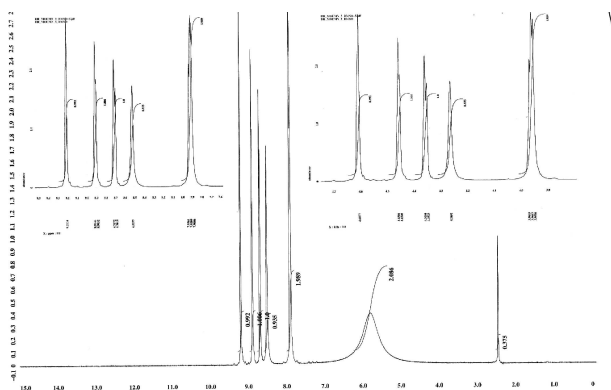Fig. 7. ^{1}H-NMR spectrum of $[Se(Nic)_4]\cdot H_2O$ complex.

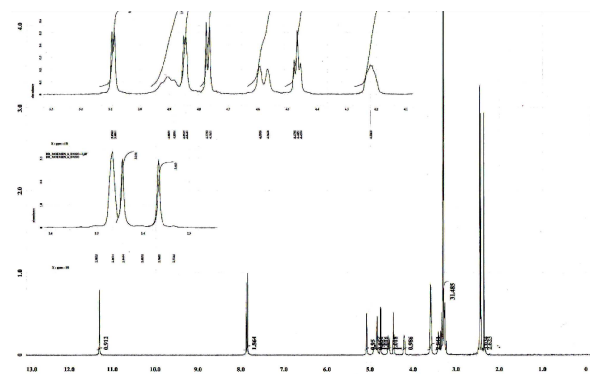Fig. 8. ^{1}H-NMR spectrum of $[Se(RF)_2]$ complex.

at $\delta = 11.32$, these results confirm that the RF coordinated to selenium metal through –N and –O atom of pyrimidine-2,4-dione moiety and the –N of –NH imide group far away of chelation. The large peak at 2.50 ppm belongs to DMSO.

3.5. Thermal analyses

The TG curves for the $[Se(Nic)_4]\cdot H_2O$ and $[Se(RF)_2]$ complexes are shown in Fig. 9. Based on the TG curve, the following mass loss sequences can be proposed concerning $[Se(Nic)_4]\cdot H_2O$ complex. The first mass loss is associated with the release of one uncoordinated water molecule with calculated 3.07%; found 2.66% at $DTG_{max} = 76\,^\circ C$. The release of uncoordinated water molecule is followed by the release of four Nic molecules with calculated 83.44%; found 83.93% at $DTG_{max} = 300\,^\circ C$. The selenium metal is a final degradation with calculated 13.49%; found 13.41%.

It is clearly obviously that for the TG curve of the $[Se(RF)_2]$ complex there does not exist any mass loss up to $200\,^\circ C$, which is interpreted as the thermal stability. At $320\,^\circ C$, this complex lost two riboflavin (RF) molecules with calculated 84.74%; found 84.10%. The final decomposition product is selenium metal contaminated with four carbon atoms as a solid residual with calculated 15.26%; found 15.90%.

The thermodynamic activation data are summarized in Table IV. The activation energies of decomposition were found to be in the range 125–181 kJ mol^{-1}. The high
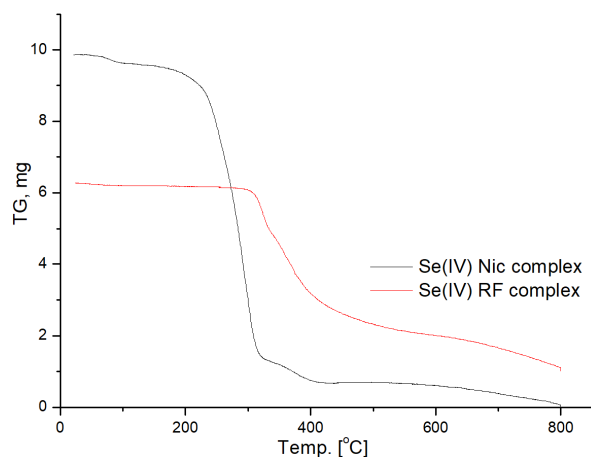

Fig. 9. TGA diagrams of Se(IV)Nic and Se(IV)RF complexes.

values of the activation energies reflect the thermal stability of the complexes [40–44]. The entropy of activation was found to have negative values in all the complexes which indicate that the decomposition reactions proceed with a lower rate than the normal ones.

TABLE IV

Thermodynamic parameters of the A $[Se(Nic)_4]\cdot H_2O$ and B $[Se(RF)_2]$ complexes.

	Parameter					
	E [kJ mol^{-1}]	A [s^{-1}]	ΔS [J mol^{-1}K^{-1}]	ΔH [kJ mol^{-1}]	ΔG [kJ mol^{-1}]	r
A	125	1.62×10^{10}	−54	121	149	0.9904
B	181	-4.97×10^{13}	−12	175	168	0.9957

3.6. X-ray powder diffraction and SEM studies

The XRD diffraction patterns within the $0^\circ < 2\theta < 80^\circ$ range for the $[Se(Nic)_4]\cdot H_2O$ and $[Se(RF)_2]$ complexes were carried out in order to obtain an idea about the lattice dynamics of these complexes (Figs. 10 and 11). All definite peaks of Se metal, Nic and RF are indexed, which are matched and compared with the standard data. The
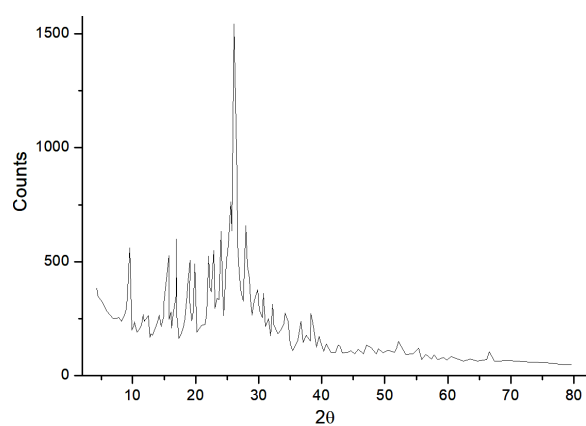

Fig. 10. XRD patterns of $[Se(Nic)_4]\cdot H_2O$.

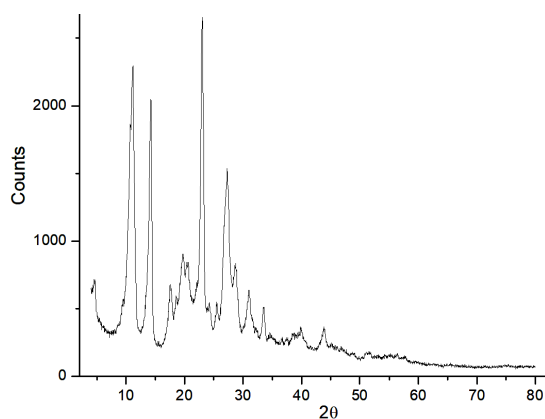Fig. 11. XRD patterns of $[Se(RF)_2]$ complex.
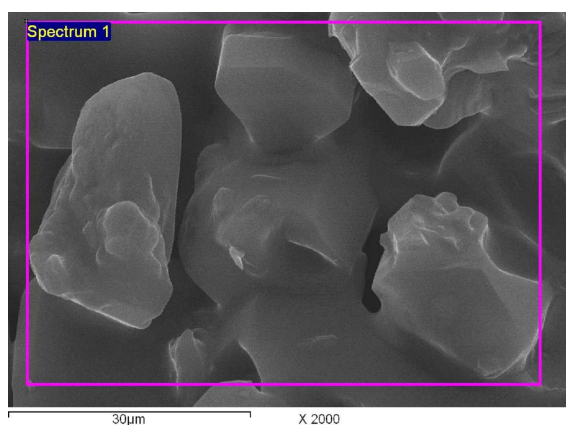
Fig. 12. SEM photo of $[Se(Nic)_4]\cdot H_2O$ complex.
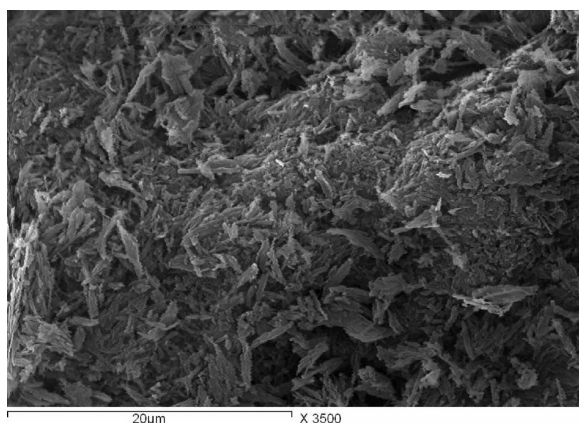

Fig. 13. SEM photo of $[Se(RF)_2]$ complex.

grain size for nanocompounds were calculated according to the Scherrer formula [45].

Purity and morphology of the nicotinamide and riboflavin selenium complexes obtained were studied using SEM to confirm the fact that each solid represents a definite compound of a definite structure which is not contaminated with starting materials. The obtained SEM micrographs, shown in Figs. 12 and 13, is allowed to verify that these complexes are the ones with the well formed

crystalline shapes. Such facts are in agreement with the formation of new complexes and were supported by the XRD data.

3.7. Antioxidant activity

The potential antioxidant activity of the tested samples was determined on the basis of three methods, the scavenging activity of the stable free radical DPPH (EC_{50} value); inhibition of the coupled oxidation of linoleic acid and beta-carotene (AA % value) and ferric reducing antioxidant power (EC_1 value). Since the reaction followed a concentration-dependent pattern, only values of EC_{50}; AA% and EC_1 of each sample; BHT and Trolox are presented in Table V. In general, the lower the EC_{50} value the higher then free radical scavenging activity of a sample. The selenium complexes of Nic and RF had significantly lower EC_{50} value compared to trolox and BHT. Regarding the EC_1 values, the lower EC_1 value the higher the ferric reducing activity of the sample. In present study, the Nic and RF selenium samples had significantly higher activity and lower EC_1 than trolox (8.35 ± 0.12 $\mu g/ml$) and BHT (4.61 ± 0.35 µg/ml). In the β-carotene linoleic acid system assay, Nic and RF complexes also possessed better antioxidant activity than trolox ($54.31 \pm 2.51\%$) and BHT ($90.20 \pm 1.81\%$). The tested complexes $[Se(Nic)_4]\cdot H_2O$ and $[Se(RF)_2]$ showed significant higher radical scavenging activity compared to butylated hydroxyanisole (BHA) (positive control), as shown in Table V. The efficiency of an antioxidant component to reduce DPPH essentially depends on its hydrogen donating ability, which is directly related to the chemical composition of each compound. In the β-carotene linoleic acid system assay, selenium complexes have ability to block the chain reaction of lipid peroxidation mainly by scavenging the intermediate lipid peroxyl radicals which are generated [29].

TABLE V

Antioxidants activities of the BHA as positive control, selenium complexes, BHT and trolox samples.

Sample	EC_{50} [µg/ml]	EC_1 [µg/ml]	AA [%]
BHA (Ve control)	1.91 ± 0.09^a	1.01 ± 0.15^a	16.26 ± 2.31^a
Nic	7.83 ± 1.13^b	3.43 ± 0.17^b	24.11 ± 0.81^b
RF	$3.88 \pm 1.02^{c,e}$	3.38 ± 0.61^e	39.44 ± 2.72^e
$[Se(Nic)_4].H_2O$	8.11 ± 0.09^b	2.91 ± 0.25^b	25.73 ± 1.91^b
$[Se(RF)_2]$	$-4.11 \pm 0.17^{c,e}$	3.91 ± 0.23^e	41.73 ± 3.01^e
BHT	21.51 ± 1.61^f	$-4.61 \pm 0.35^{b,c}$	90.20 ± 1.81^f
trolox	$6.75 \pm 0.22^{c,g}$	8.35 ± 0.12^f	54.31 ± 2.51^g

[a,b,c,d] data bearing different superscript letters in the same raw were significantly different ($P < 0.05$). Each value is presented as means±standard deviation ($n = 3$).

4. Conclusion

This paper discussed the preparation and characterization of two new selenium(IV) complexes with nicotinamide and riboflavin vitamins. This research aimed to some items as addressing some of the vitamin drugs containing selenium as one of the important elements to reduce the free radicals, preparation of a selenium compounds in the nanometric form which gave a great impor-

tance in increase of the efficiency of absorption of human cells to selenium while minimizing the amount of active ingredient (i.e., higher absorption and less amount), and reduce the side effects of chemical additives. This paper gives a new idea to the pharmaceutical companies through the preparation of selenium and its compounds in the nanometric form which facilitates human cells to absorbed quickly and efficiently rather than large dose, which gives high efficiency of the vital force to increase the body immune system. Screening of antioxidant activities of selenium(IV) complexes in *vitro* were investigated. The antioxidant activity was studied by three methods (DPPH assay; β-carotene/linoleic acid a bleaching assay and ferric reducing power assay. The studied Se(IV) complexes have a significant higher antioxidant activity compared to synthetic antioxidants like trolox and BHT.

References

[1] J.D. Odom, W.H. Dawson, P.D. Ellis, *J. Am. Chem. Soc.* **101**, 5815 (1979).

[2] H. Robberecht, H. Deelstra, *Talanta* **31**, 49 (1984).

[3] R.W. Andrews, D.C. Johnson, *Anal. Chem.* **47**, 259 (1975).

[4] M.E. El-Boshy, E.F. Risha, F.M. Abdelhamid, M.S. Mubarak, T.B. Hadda, *J. Trace Element Med. Biol.* **29**, 104 (2015).

[5] J. Pieczynska, H. Grajeta, *J. Trace Element Med. Biol.* **29**, 31 (2015).

[6] M. Vinceti, P. Grill, C. Malagoli, T. Filippini, S. Storani, M. Malavolti, B. Michalke, *J. Trace Elem. Med. Biol.* **31**, 1 (2015).

[7] B. Corvilain, B. Contempre, A.O. Longombe, P. Goyens, C. Gervy-Decoster, F. Lamy, J.B. Vanderpas, J.E. Dumont, *Am. J. Clin. Nutr.* **57**, 244S (1993).

[8] P. Drevensek, T. Zupancic, B. Pihlar, R. Jerala, U. Kolitsch, A. Plaper, I. Turel, *J. Inorg. Biochem.* **99**, 432 (2005).

[9] J.H. He, D.R. Xiao, H.Y. Chen, S.W. Yan, D.Z. Sun, X. Wang, J. Yang, R. Yuan, E.B. Wang, *Inorg. Chim. Acta* **385**, 170 (2012).

[10] L. Kathawate, S. Sproules, O. Pawar, G. Markad, S. Haram, V. Puranik, S. Salunke-Gawali, *J. Mol. Str.* **1048**, 223 (2013).

[11] *Metallotherapeutic Drugs and Metal-Based Diagnostic Agents, the Use of Metals in Medicine*, Eds. M. Gielen, E.R.T. Tiekink, Wiley, Chichester 2005.

[12] M.P. López-Gresa, R. Ortiz, L. Perelló, J. Latorre, M. Liu-González, S. Garcıa-Granda, M. Pérez-Priede, E. Cantón, *J. Inorg. Biochem.* **92**, 65 (2002).

[13] D.R. Xiao, E.B. Wang, H.Y. An, Y.G. Li, L. Xu, *Cryst. Growth Des.* **7**, 506 (2007).

[14] D.R. Xiao, J.H. He, D.Z. Sun, H.Y. Chen, S.W. Yan, X. Wang, J. Yang, R. Yuan, E.B. Wang, *Eur. J. Inorg. Chem.* **11**, 1783 (2012).

[15] N.M. Niren, *Pharmacologic doses of nicotinamide in the treatment of inflammatory skin conditions: a review*, Cutis 77 (1 Suppl): 11–6 (2006).

[16] Wikipedia, *Nicotinamide*.

[17] C.R. Bondy, P.A. Gale, S.J. Loeb, *Chem. Commun.* **8**, 729 (2001).

[18] V.A. Sharnin, S.V. Dushina, M.A. Zevakin, A.S. Gushchina, K.V. Grazhdan, *Inorg. Chim. Acta* **362**, 437 (2009).

[19] R.L. Lieberman, A. Bino, N. Mirsky, D.A. Summers, R.C. Thompson, *Inorg. Chim. Acta* **297**, 1 (2000).

[20] B. Kozlevcar, I. Leban, I. Turel, P. Segedin, M. Petric, F. Pohleven, A.J.P. White, D.J. Williams, J. Sieler, *Polyhedron* **18**, 755 (1999).

[21] M. Melnik, J. Mrozinski, C.E. Holloway, *J. Coord. Chem.* **29**, 209 (1993).

[22] I. Uçar, A. Bulut, A. Karadağ, C. Kazak, *J. Mol. Struct.* **837**, 38 (2007).

[23] E. Şahin, S. İde, A. Ataç, Ş. Yurdakul, *J. Mol. Struct.* **616**, 253 (2002).

[24] A. Atac, S. Yurdakul, S. Berber, *Spectrochim. Acta A* **81**, 684 (2011).

[25] S. Swavey, E.S. Gould, *Inorg. Chem.* **39**, 352 (2000).

[26] C.N. Malele, J. Ray, W.E. Jones Jr, *Polyhedron* **29**, 749 (2009).

[27] A.N. Singh, E. Gelerinter, E.S. Gould, *Inorg. Chem.* **21**, 1232 (1982).

[28] O.P. Sharma, T.K. Bhat, *Food Chem.* **113**, 1202 (2009).

[29] H. Miraliakbari, F. Shahidi, *Food Chem.* **111**, 421 (2008).

[30] G. Ozkan, O. Sagdic, S. Gokturk, O. Unal, S. Albayrak, *Food Sci. Technol.* **43**, 186 (2010).

[31] A.W. Coats, J.P. Redfern, *Nature* **201**, 68 (1964).

[32] W.J. Geary, *Coord. Chem. Rev.* **7**, 81 (1971).

[33] K. Nakamoto, *Infrared and Raman Spectra of Inorganic and Coordination compounds*, 3rd ed., Wiley Interscience, New York 1978.

[34] H.L. Singh, A.K. Vershney, *Bioinorg. Chem. Appl.* **2006**, 1 (2006).

[35] O.F. Ozturk, M. Sekerci, E. Ozdemir, *Russ. J. Coord. Chem.* **31**, 687 (2005).

[36] O.F. Ozturk, M. Sekerci, E. Ozdemir, *Russ. J. Gen. Chem.* **76**, 36 (2006).

[37] A. Atac, S. Yurdakul, S. Berber, *Spectrochim. Acta A* **81**, 684 (2011).

[38] J.R. Allan, N.D. Baird, A.L. Kassyk, *J. Therm. Anal.* **16**, 79 (1979).

[39] A.H. Beckett, J.B. Stenlake, *Pharmaceutical Chemistry Quantitative Analysis*, Athlone Press, London 1962, p. 301.

[40] P. Scherrer, *Göttinger Nachrichten Gesell.* **2**, 98 (1918) (in German).

[41] M.M. Omar, *J. Therm. Anal. Calc.* **96**, 607 (2009).

[42] A. Rotaru, M. Goşa, P. Rotaru, *J. Therm. Anal. Calc.* **94**, 367 (2008).

[43] R.K. Verma, L. Verma, A. Bhushan, B.P. Verma, *J. Therm. Anal. Calc.* **90**, 725 (2007).

[44] M.S. Refat, I.M. El-Deen, Z.M. Anwer, S. El-Ghol, *J. Mol. Struct.* **920**, 149 (2009).

[45] M.S. Refat, I.M. El-Deen, Z.M. Anwer, S. El-Ghol, *J. Coord. Chem.* **62**, 1709 (2009).